Reversible Binding of Nitric Oxide to Tyrosyl Radicals in Photosystem II. Nitric Oxide Quenches Formation of the S3 EPR Signal Species in Acetate-Inhibited Photosystem II[†]

Veronika A. Szalai and Gary W. Brudvig*

Department of Chemistry, Yale University, New Haven, Connecticut 06511

Received May 10, 1996; Revised Manuscript Received July 23, 1996[⊗]

ABSTRACT: Continuous illumination at temperatures above 250 K of photosystem II samples which have been depleted of calcium or chloride or treated with fluoride, acetate, or ammonia results in production of a broad radical EPR signal centered at $g = 2.0$. This EPR signal, called the S3 EPR signal, has been attributed to an organic radical interacting with the S_2 state of the oxygen-evolving complex to give the species S_2X^+ (X^+ = organic radical). A tyrosine radical has been proposed as the species responsible for the S3 EPR signal. On the basis of experiments demonstrating that nitric oxide binds reversibly to the tyrosyl radical in ribonucleotide reductase, nitric oxide has been used to probe the S3 EPR signal in acetate-treated photosystem II. In experiments using manganese-depleted photosystem II, nitric oxide was found to bind reversibly to both redox-active tyrosines, $Y_D^\bullet$ and $Y_Z^\bullet$, to form EPR-silent adducts. Next, acetate-treated photosystem II was illuminated to form the S3 EPR signal in the presence of nitric oxide to test whether the S3 EPR signal behaves like $Y_Z^\bullet$. Under conditions that produce the maximum yield of the S3 EPR signal in acetate-treated photosystem II, no S3 EPR signal was observed in the presence of nitric oxide. Upon removal of nitric oxide, the S3 EPR signal could be induced. Quenching of the S3 EPR signal by nitric oxide yielded an S_2-state multiline EPR signal. Its amplitude was 45% of that found for uninhibited photosystem II illuminated at 200 K; this yield is the same as the yield of the S3 EPR signal under equivalent conditions but without nitric oxide. These results suggest that the S3 EPR signal is due to the configuration $S_2Y_Z^\bullet$ in which the S_2 state of the oxygen-evolving complex gives a broadened multiline EPR signal as a result of exchange and dipolar interactions with $Y_Z^\bullet$. The binding of nitric oxide to $Y_Z^\bullet$ to form a diamagnetic Y_Z−NO species uncouples the S_2 state from $Y_Z^\bullet$, yielding a noninteracting S_2-state multiline EPR signal species.

Photosystem II (PSII)[1] is the protein complex in green plants responsible for the light-driven oxidation of water to dioxygen and the reduction of plastoquinone to plastoquinol [for reviews, see Debus (1992), Ghanotakis and Yocum (1990), and Rutherford et al. (1992)]. To produce dioxygen, the OEC, a tetranuclear manganese−oxo complex, is photooxidized four times and cycles through five "store" or S states labeled S_0−S_4 (Kok et al., 1970). The oxidations associated with each S-state transition may be strictly due to oxidations of the Mn_4 cluster (Dekker et al., 1984b; Ono et al., 1992) or to the oxidation of the Mn_4 cluster and a nearby organic radical (Boussac et al., 1989, 1990; Guiles et al., 1990; Nugent et al., 1993).

PSII samples that have been depleted of calcium or chloride or treated with fluoride, acetate, or ammonia can no longer cycle through all of the S states (Andréasson & Lindberg, 1992; Baumgarten et al., 1990; Boussac & Rutherford, 1988; MacLachlan & Nugent, 1993). When these samples are continuously illuminated at temperatures above 250 K, a broad EPR signal, known as the S3 EPR signal, is observed centered at $g = 2.0$ (Boussac et al., 1989). On the basis of flash experiments (Baumgarten et al., 1990; Boussac et al., 1990; Szalai & Brudvig, 1996), EPR spectroscopy (Baumgarten et al., 1990; Boussac et al., 1990; Sivaraja et al., 1989; Szalai & Brudvig, 1996), and X-ray absorption studies (Guiles et al., 1990; Nugent et al., 1993), the S3 EPR signal is proposed to arise from weak exchange and dipolar coupling of an organic radical with the S_2 state of the Mn_4 cluster to give the configuration S_2X^+ (X^+ = organic radical). Spin-echo detected ENDOR studies of the S3 EPR signal from calcium-depleted PSII (Gilchrist et al., 1995) and ESEEM experiments on *Synechocystis* PSII samples isotopically labeled at tyrosine (Tang et al., 1996a) show that $Y_Z^\bullet$ is the species responsible for the S3 EPR signal.

In untreated PSII, $Y_Z^\bullet$ is the direct oxidant of the OEC and is reduced with microsecond to millisecond half-times depending on the S state of the OEC (Hoganson & Babcock, 1988). However, in manganese-depleted samples, $Y_Z^\bullet$ decays less quickly and can be trapped by continuous illumination at 0 °C followed by freezing under illumination to 200 K (Tang et al., 1996b). Because $Y_Z^\bullet$ is the primary oxidant of

[†] This work was supported by the National Institutes of Health (GM 32715) and by a National Institutes of Health predoctoral traineeship to V.A.S. (GM 08283).

[⊗] Abstract published in *Advance ACS Abstracts,* November 1, 1996.

[1] Abbreviations: chl, chlorophyll; DCMU, 3-(3,4-dichlorophenyl)-1,1-dimethylurea; DMSO, dimethyl sulfoxide; EDTA, ethylenediaminetetraacetic acid; ENDOR, electron nuclear double resonance; EPR, electron paramagnetic resonance; ESEEM, electron spin echo envelope modulation; MES, 2-morpholinoethanesulfonic acid; NO•, nitric oxide; OEC, O_2-evolving complex; PPBQ, phenyl-*p*-benzoquinone; P680, chlorophyll primary electron donor in PSII; PSII, photosystem II; Q_A, tightly bound plastoquinone in PSII; Q_B, exchangeable plastoquinone in PSII; Tris, tris(hydroxymethyl)aminomethane; Y_D, tyrosine 160 of the D2 polypeptide; Y_Z, tyrosine 161 of the D1 polypeptide.

S0006-2960(96)01117-8 CCC: $12.00

the OEC, treatments which affect electron and/or proton transfer reactions to and from the OEC could also affect the stability of $Y_Z^{\bullet}$. Acetate treatment of PSII is believed to inhibit O_2-evolution by competing with chloride for a binding site near the OEC (MacLachlan & Nugent, 1993; Sinclair, 1984). By blocking OEC turnover, acetate treatment may produce conditions which stabilize $Y_Z^{\bullet}$ and explain why $Y_Z^{\bullet}$ is the species responsible for the S3 EPR signal.

Recently, it has been reported that nitric oxide binds reversibly to hindered phenoxy radicals (Janzen et al., 1993; Wilcox & Janzen, 1993) and to the tyrosyl radical in ribonucleotide reductase (Lepoivre et al., 1992; Roy et al., 1995). In previous experiments with oxygen-evolving PSII, nitric oxide was found to bind to the non-heme Fe(II) and to eliminate the EPR signal of $Y_D^{\bullet}$ (Petrouleas & Diner, 1990). The disappearance of the $Y_D^{\bullet}$ EPR signal is evidence for formation of an adduct between $NO^{\bullet}$ and $Y_D^{\bullet}$.

Nitric oxide also binds to cysteine residues forming S-nitrosylated species under aerobic conditions (De Groote et al., 1995; Gaston et al., 1993; Jia et al., 1996; Stamler et al., 1992a,b). The D1 and D2 subunits of PSII only contain three conserved cysteine residues (D1-Cys 18, D2-Cys 41, D2-Cys 212) (Svensson et al., 1991), all on the stromal side of the membrane, and their reaction with $NO^{\bullet}$ would not be expected to affect the donor-side reactions. However, the 33 kDa extrinsic polypeptide, known as the Mn-stabilizing protein, contains a disulfide linkage which could react with $NO^{\bullet}$ to form S-nitrosylated species. It has been observed that the 33 kDa protein cannot bind to PSII upon cleavage of the disulfide linkage (Tanaka & Wada, 1988); dissociation of the 33 kDa subunit leads to manganese release from the OEC unless high chloride concentrations are maintained (Miyao & Murata, 1984). Since no free manganese was reported by Petrouleas and Diner (1990) upon addition of $NO^{\bullet}$ to PSII samples, it seems unlikely that this reaction occurs to any significant degree. This is also consistent with the observation that nitric oxide had no effect on the S_1 to S_2 transition of the OEC at concentrations below 300 μM (Petrouleas & Diner, 1990).

In our experiments, manganese-depleted PSII was treated with nitric oxide and the EPR signal of $Y_D^{\bullet}$ was reversibly quenched in the dark. When an identical sample was illuminated under conditions known to produce high yields of $Y_Z^{\bullet}$ (Tang et al., 1996b), $Y_Z^{\bullet}$ was not observed because of rapid formation of the diamagnetic adduct Y_Z−NO. Removal of $NO^{\bullet}$ in the dark, followed by reillumination, produced the EPR signal from $Y_Z^{\bullet}$. When acetate- and nitric oxide-treated PSII was illuminated to produce the maximum yield of the S3 EPR signal (Szalai & Brudvig, 1996), no S3 EPR signal was observed. Instead, quenching of the S3 EPR signal removed the exchange and dipolar coupling between the S3 EPR signal species and the S_2 state and allowed observation of an S_2-state multiline EPR signal. Its amplitude was 45% of that found for a DCMU-treated PSII sample; this yield is the same as the yield of the S3 EPR signal under equivalent conditions but without nitric oxide. Upon removal of nitric oxide, the S3 EPR signal could be induced. These results suggest that the S3 EPR signal is due to the configuration $S_2Y_Z^{\bullet}$ and that it is the multiline form of the S_2 state of the OEC which is responsible for broadening the $Y_Z^{\bullet}$ EPR signal to give the S3 EPR signal.

MATERIALS AND METHODS

MES was purchased from Sigma. Ethylene glycol, DMSO, and sucrose were purchased from Baker and used without further purification. Anhydrous sodium acetate was purchased from Fisher Chemical, and sodium chloride was purchased from Mallinckrodt. DCMU was purchased from Sigma and recrystallized twice from ethanol. Nitric oxide was purchased from Union Carbide and was purified by condensing approximately 1 atm of the impure $NO^{\bullet}$ to 77 K on a vacuum line and then subliming it to collect the colorless nitric oxide. The purified nitric oxide was stored in glass bulbs equipped with vacuum adapters until use.

PSII membranes were isolated from market spinach leaves following the procedure of Berthold et al. (1981) with the modifications of Beck et al. (1985) except that thylakoid membranes were not frozen to 77 K before isolation of PSII membranes. The PSII membranes were stored at 77 K in resuspension buffer [15 mM NaCl, 20 mM MES, 30% (v/v) ethylene glycol at pH 6.0] at chlorophyll concentrations of approximately 6−8 mg of chl/mL until use. Chlorophyll concentrations were measured according to the method of Arnon (1949) on a Perkin-Elmer Lambda 3b Series UV−vis spectrophotometer. Typical oxygen-evolution rates were 350−400 μmol of O_2 (mg of chl)$^{-1}$ h^{-1} for untreated PSII as measured by a Clarke electrode using the method presented in Beck et al. (1985).

Acetate-treated samples were prepared as in Szalai and Brudvig (1996). Manganese-depleted PSII membranes were prepared by 5 mM hydroxylamine treatment as in Tamura and Cheniae (1987). Experiments with nitric oxide required that the full amplitude of $Y_D^{\bullet}$ be present before equilibration with $NO^{\bullet}$. Since the yield of photo-oxidation of Y_D increases with increasing pH, manganese-depleted PSII (0.6 mL) was resuspended in pH 7.5 buffer containing 20 mM HEPES, 15 mM NaCl, and 30% ethylene glycol (v/v) to a final chlorophyll concentration of 6−8 mg/mL (Buser & Brudvig, 1992).

After being transferred to EPR tubes, PPBQ (Aldrich, 25 mM stock solution in DMSO) was added to the acetate-treated PSII to give a final concentration of 500 μM. The samples were incubated in the dark at 0 °C for 30−60 min, and then they were frozen to 77 K in the dark. For acetate- and DCMU-treated samples, $K_3Fe(CN)_6$ (Mallinckrodt, 10 mM stock solution in water) was added to oxidize any dark-reduced Q_A. The final concentration of ferricyanide was 200 μM. The samples were thoroughly stirred and allowed to incubate for 30 min at 0 °C before DCMU (10 mM solution in DMSO) was added in the dark to a final concentration of 200 μM. The samples were incubated for another 30 min at 0 °C before being frozen to 77 K in the dark. $K_3Fe(CN)_6$ was added to manganese-depleted PSII to give a final concentration of 200 μM.

Before $NO^{\bullet}$ was added, manganese-depleted samples were preilluminated for 3−5 min at 0 °C to induce the full yield of $Y_D^{\bullet}$. For studies of $NO^{\bullet}$ binding to $Y_Z^{\bullet}$ or the S3 EPR signal species, the samples were illuminated after addition of $NO^{\bullet}$. The illumination conditions to produce $Y_Z^{\bullet}$ were similar to those presented by Tang et al. (1996b). However, to avoid photo-oxidation of chl_Z (Thompson & Brudvig, 1988), we froze the sample under illumination to 200 K in a dry ice/ethanol bath before freezing it in darkness to 77 K. The S3 EPR signal was produced by continuous

illumination for 5 s at room temperature (294 K) followed by freezing to 77 K. In DCMU-treated PSII at pH 6.0, the S_2-state multiline EPR signal was produced by 10 min of continuous illumination at 200 K. DCMU- and acetate-treated PSII samples were illuminated at 230 K (acetonitrile/dry ice), 250 K (carbon tetrachloride/dry ice), 258 K (ethylene glycol/dry ice), or 273 K. Continuous illuminations were performed with a quartz halogen lamp (700 W/m^2).

Samples for NO$^\bullet$ experiments were degassed by using two freeze−pump−thaw cycles on a vacuum line; this procedure generally took 15−25 min. The samples were frozen to 200 K (dry ice/acetone bath) and dinitrogen was introduced before thawing to prevent bumping of the samples. After the final cycle, the samples were frozen to 200 K and nitric oxide, 0.039 atm for manganese-depleted samples and 0.132 atm for acetate-treated samples, was introduced. No difference in sample behavior was observed over the range of nitric oxide concentrations used. After NO$^\bullet$ was removed from the rest of the vacuum line, the EPR tube head space was filled with dinitrogen to keep the total pressure at approximately 1 atm. Nitric oxide was equilibrated into the sample by thawing the sample to 0 °C in the dark, allowing the sample to coat the inside of the EPR tube, and rotating the sample for 2−3 min. After the sample was allowed to flow to the bottom of the EPR tube, the mixing process was repeated. After two mixing cycles, the sample was frozen to 77 K.

Low-temperature EPR spectroscopic measurements were performed on a Varian E-line EPR spectrometer equipped with an Oxford Instruments ESR 900 liquid helium cryostat with the following conditions unless otherwise noted: microwave frequency, 9.28 GHz; microwave power, 5 mW (S3 and S_2-state EPR signals) or 0.1 mW (tyrosine radical EPR signals); magnetic field modulation frequency, 100 kHz; magnetic field modulation amplitude, 20 G (S3 and S_2-state EPR signals) or 5 G (tyrosine radical EPR signals); temperature, 6 K. Matched samples for EPR spectroscopy were prepared with and without nitric oxide. The intensity of the rhombic iron EPR signal at $g = 4.3$ was used for scaling spectra before nitric oxide was added. The S_2-state multiline EPR signal intensity was approximated as the sum of 4−8 hyperfine peak heights. The S_2-state $g = 4.1$ EPR signal peak height was measured in light-minus-dark difference spectra. The percentage of centers producing $Y_Z^\bullet$ was obtained by comparing the total integrated area of the spectrum of $Y_D^\bullet$ to the total integrated area of the spectrum containing both $Y_D^\bullet$ and $Y_Z^\bullet$. The area of $Y_D^\bullet$ was subtracted to give the amount of $Y_Z^\bullet$.

RESULTS

Binding of NO$^\bullet$ to $Y_D^\bullet$. Previous experiments using oxygen-evolving PSII membranes indicated that the EPR signal from $Y_D^\bullet$ could be reversibly quenched upon introduction of a mixture of nitrogen and NO$^\bullet$ (Petrouleas & Diner, 1990). The dissociation constant for binding of NO$^\bullet$ to $Y_D^\bullet$ was estimated to be 3 μM based on a titration of the disappearance of the $Y_D^\bullet$ EPR signal with increasing NO$^\bullet$ concentration (Petrouleas & Diner, 1990). Removal of NO$^\bullet$ by evacuation of the sample regenerated the EPR signal from $Y_D^\bullet$.

As a control to confirm that NO$^\bullet$ bound reversibly to $Y_D^\bullet$ in manganese-depleted samples, EPR spectra were collected

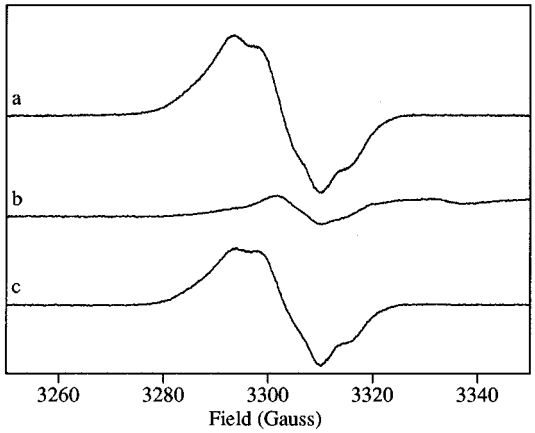

FIGURE 1: Effect of nitric oxide on the EPR signal of $Y_D^\bullet$ in manganese-depleted PSII: spectrum (a) before nitric oxide added, (b) after nitric oxide added, and (c) after nitric oxide removed. EPR spectrometer and sample conditions for all of the figures are given in the Materials and Methods section of the text.

both before and after NO$^\bullet$ had been mixed into the sample (Figure 1). As shown in Figure 1b, incubation with NO$^\bullet$ replaced the EPR signal of $Y_D^\bullet$ with a small EPR signal at $g = 2.0$. This EPR signal was probably due to oxidized chl_Z (Thompson & Brudvig, 1988) formed by exposure of the sample to small amounts of light at 77 K. It was only produced in a small number of centers since its integrated area corresponded to only 5% of the total integrated area of the EPR spectrum of $Y_D^\bullet$. After NO$^\bullet$ had been removed, the amount of $Y_D^\bullet$ present was 92% of that observed before NO$^\bullet$ had been added (Figure 1c). This means that very little $Y_D^\bullet$ EPR signal intensity was lost upon removal of NO$^\bullet$ (Figure 1a,c) and confirms that reversible NO$^\bullet$ binding to $Y_D^\bullet$ occurs without chemical reduction of $Y_D^\bullet$. To obtain a reliable estimate of the amount of $Y_D^\bullet$ present, the sample was illuminated after NO$^\bullet$ removal to induce any $Y_D^\bullet$ lost during the freeze−pump−thaw manipulations. Taking the yield of $Y_D^\bullet$ induced after NO$^\bullet$ removal as 100%, the amount of $Y_D^\bullet$ present before NO$^\bullet$ was added (Figure 1a) can be calculated to be 75%. This 25% difference in the intensity of the EPR signal from $Y_D^\bullet$ was probably due to decay of $Y_D^\bullet$ during the time required to degas and introduce NO$^\bullet$ into the sample.

Binding of NO$^\bullet$ to $Y_Z^\bullet$. In oxygen-evolving PSII, $Y_Z^\bullet$ is transiently formed as an unstable intermediate and is rapidly reduced by the OEC. Therefore, quantitative trapping of $Y_Z^\bullet$ can only be achieved when the oxygen-evolving complex has been either removed or inhibited. By freezing under illumination, $Y_Z^\bullet$ has been trapped in high yield in the D2-Tyr160Phe mutant of *Synechocystis* P6803 (Tang et al., 1996b). We repeated the $Y_Z^\bullet$-trapping experiments described in Tang et al. (1996b), but used manganese-depleted PSII membranes instead. In a manganese-depleted sample treated with ferricyanide, 86% of the full yield of $Y_Z^\bullet$ could be obtained relative to the full amplitude of $Y_D^\bullet$ (Figure 2b). Dark incubation for 10 s at 0 °C allowed the trapped $Y_Z^\bullet$ to decay and resulted in the same amplitude of $Y_D^\bullet$ being recovered as had been initially induced by 5 min of continuous illumination at 0 °C. When an identical manganese-depleted sample was degassed, incubated with NO$^\bullet$, and illuminated to trap $Y_Z^\bullet$, no EPR signal due to $Y_Z^\bullet$ was observed (Figure 2c). It was also observed that the free NO$^\bullet$ EPR signal decreased after illumination by an amount

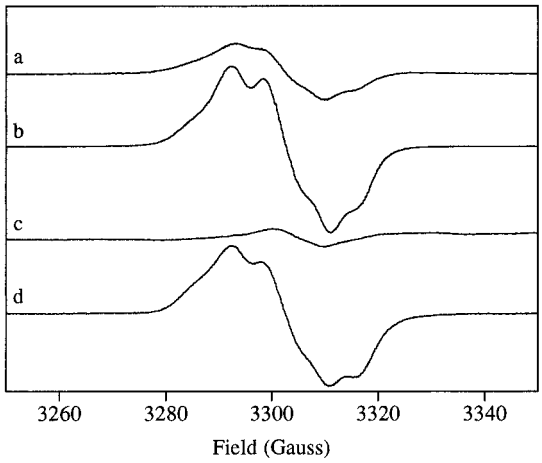

FIGURE 2: Effect of nitric oxide on the EPR signal of $Y_Z^\bullet$ in manganese-depleted PSII: spectrum (a) $Y_D^\bullet$ before NO$^\bullet$ added, (b) illumination (see text) to produce $Y_Z^\bullet$ without NO$^\bullet$, (c) illumination to produce $Y_Z^\bullet$ after addition of NO$^\bullet$, and (d) illumination to produce $Y_Z^\bullet$ after removal of NO$^\bullet$.

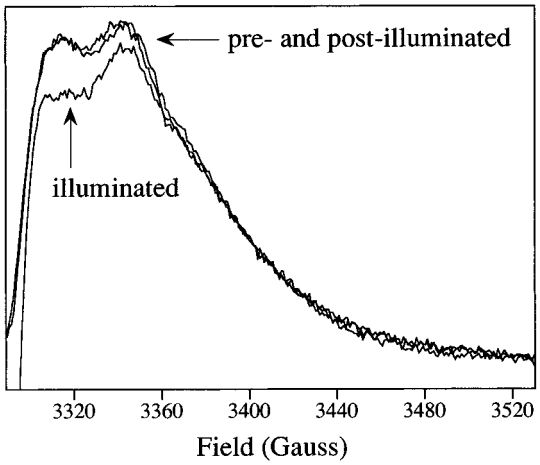

FIGURE 3: Decrease in the concentration of free NO$^\bullet$ upon illumination to produce $Y_Z^\bullet$ in manganese-depleted PSII. The preilluminated spectrum was recorded after 15 min of dark incubation with NO$^\bullet$ at 0 °C. Based on the solubility of NO$^\bullet$ in water at 25 °C, the sample contains approximately 0.1 mM free NO$^\bullet$, although the free NO$^\bullet$ concentration is expected to be somewhat higher in detergent solutions. The illuminated spectrum was recorded after illumination (see text) to produce $Y_Z^\bullet$. The postilluminated spectrum was recorded after 15 min of dark incubation at 0 °C, [Chl] = 4.7 mg/mL, and EPR spectra were measured at 10 K.

consistent with NO$^\bullet$ binding to $Y_Z^\bullet$ and that, upon dark incubation of the sample at 0 °C, the initial intensity of the NO$^\bullet$ EPR signal was restored (Figure 3). After several cycles of illumination followed by dark incubation, the free NO$^\bullet$ concentration did not progressively decrease, indicating that PSII does not photochemically consume NO$^\bullet$. Upon illumination to produce $Y_Z^\bullet$, the EPR signal from the Fe(II)−NO adduct disappeared, indicating that charge-separation had taken place. These results indicate that Y_Z was the reductant of $P680^+$ and that, upon its oxidation, $Y_Z^\bullet$ formed a diamagnetic adduct with NO$^\bullet$. Figure 2d shows that after the NO$^\bullet$ had been removed, 76% of the full amplitude of $Y_Z^\bullet$ could be reinduced. This is almost the same yield of $Y_Z^\bullet$ observed in an untreated manganese-depleted sample.

Quenching of the S3 EPR Signal by NO$^\bullet$. The experiments on manganese-depleted PSII indicated that the EPR signal from $Y_Z^\bullet$ was not generated upon treatment with NO$^\bullet$. We

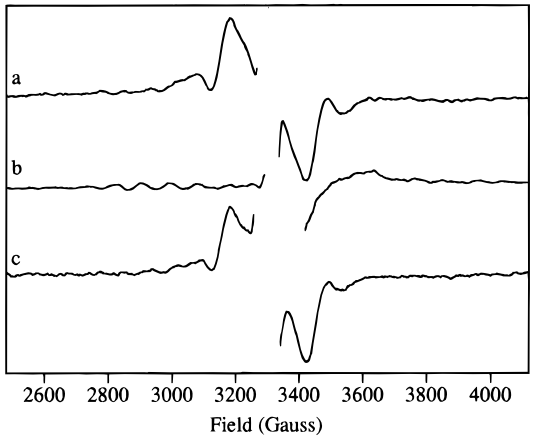

FIGURE 4: Effect of nitric oxide on the S3 EPR signal in acetate-treated PSII: spectrum (a) S3 EPR signal produced by 5 s of illumination at 294 K in acetate-treated PSII, (b) acetate-treated PSII illuminated for 5 s at 294 K after addition of NO$^\bullet$, and (c) acetate-treated PSII illuminated for 5 s at 294 K after removal of NO$^\bullet$. Spectra are light-minus-dark difference spectra, and the g = 2.0 portions of the spectra, containing the EPR signal from $Y_D^\bullet$, have been removed.

attribute this to formation of an EPR-silent Y_Z−NO adduct during illumination. The S3 EPR signal has been found to arise from a tyrosine radical interacting with the OEC (Gilchrist et al., 1995; Nugent et al., 1993; Tang et al., 1996a). Therefore, we added NO$^\bullet$ to an acetate-treated PSII sample in order to probe the nature of the S3 EPR signal species. Under illumination conditions (5 s, 294 K) which produce the maximum yield of the S3 EPR signal in acetate-treated PSII (Szalai & Brudvig, 1996), no S3 EPR signal formed when NO$^\bullet$ was present (Figure 4b). Figure 4 also demonstrates that after removal of NO$^\bullet$ the sample could be reilluminated and the S3 EPR signal could be induced. These results suggest that the S3 EPR signal species in acetate-treated PSII is suppressed by NO$^\bullet$ binding in a manner similar to that found for $Y_Z^\bullet$ in manganese-depleted samples.

Although the S3 EPR signal is thought to arise from the interaction of an organic radical with the S_2 state, S_2-state multiline or g = 4.1 EPR signals have not been observed under conditions which produce the S3 EPR signal. This is believed to be because broadening effects due to exchange and dipolar coupling in the state S_2X^+ make an EPR signal from the S_2 state unobservable. It has been reported that a broad S_2-state EPR signal is present together with the S3 EPR signal in calcium-depleted PSII (Zimmermann et al., 1993). Since one way to remove these effects is to eliminate one of the spins, we expected that quenching of the organic radical ($Y_Z^\bullet$) by formation of the diamagnetic Y_Z−NO adduct in acetate-treated PSII would produce the state S_2Y_Z−NO and make an EPR signal from the S_2 state observable. Figures 4 and 5 show that although no S3 EPR signal was observed upon illumination of acetate- and NO$^\bullet$-treated PSII, a multiline EPR signal was observed (Figure 4b and Figure 5a). Its hyperfine coupling constant was approximately 88 G, which is almost identical to that found for the S_2-state multiline EPR signal in DCMU-treated samples (see Figure 5c). Compared to the maximum intensity of the S_2-state multiline EPR signal found in a DCMU-treated PSII sample, the multiline EPR signal found in acetate- and NO$^\bullet$-treated PSII represents approximately 45% of the centers (Figure 5). Within error, this intensity corresponds to the maximum

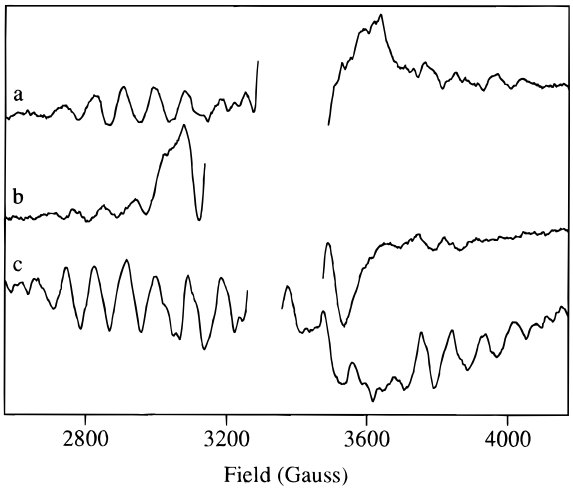

FIGURE 5: Comparison of the S_2-state multiline EPR signals produced in (a) acetate- and NO•-treated PSII illuminated for 5 s at 294 K, (b) acetate-treated PSII illuminated for 5 s at 294 K, and (c) DCMU-treated PSII illuminated for 10 min at 200 K. Spectra are light-minus-dark difference spectra. The large central peaks of the S3 EPR signal have been removed in spectrum b. All spectra have had the $g = 2.0$ regions, containing the EPR signal from Y_D•, removed for clarity.

steady-state yield of the S3 EPR signal which can be produced in acetate-treated PSII (Szalai & Brudvig, 1996). The remaining centers are probably in the $g = 4.1$ form of the S_2 state since the S3 EPR signal decays rapidly to this state. However, in the presence of NO•, a number of overlapping signals are present in the g $\approx$ 4 region which obscure the S_2-state $g = 4.1$ EPR signal. These results support our conclusion that the S3 EPR signal is due to the state S_2Y_Z• since quenching of the radical reveals an S_2-state EPR signal in an almost identical yield to that of the S3 EPR signal.

On the basis of a two-turnover requirement for production of the S3 EPR signal, these results also suggest that, if acetate-treated PSII were limited to one turnover, the S_2-state multiline EPR signal should be observed. Instead, however, an S_2-state $g = 4.1$ EPR signal has been observed from acetate-treated PSII. In single-turnover experiments on acetate-treated PSII using saturating laser-flashes, no S_2-state EPR signals were observed (Szalai & Brudvig, 1996) due to the low protein concentrations required for flash experiments which made observation of the S_2-state $g = 4.1$ EPR signal difficult. As an alternative, acetate-treated PSII can be limited to one turnover with DCMU so that observable amounts of the S_2-state EPR signals can be produced. Illumination of acetate- and DCMU-treated PSII at temperatures between 230 and 273 K produced only the $g = 4.1$ form of the S_2 state (Figure 6, inset). Figure 6 also shows that the S_1 to S_2 transition onset temperature in acetate-treated PSII is approximately 240 K. This is similar to the onset temperature of -40 °C ($\approx$230 K) reported for the S_1 to S_2 transition in calcium-depleted PSII (Ono and Inoue, 1990). A model presented by Szalai and Brudvig (1996) suggested that the S_2-state $g = 4.1$ EPR signal was involved in the formation and decay of the S3 EPR signal species in acetate-treated PSII. The model is based on the results of flash experiments demonstrating a two-flash requirement for formation of the S3 EPR signal and the observation that dark incubation of samples exhibiting the S3 EPR signal produces the S_2-state $g = 4.1$ EPR signal upon decay. While the

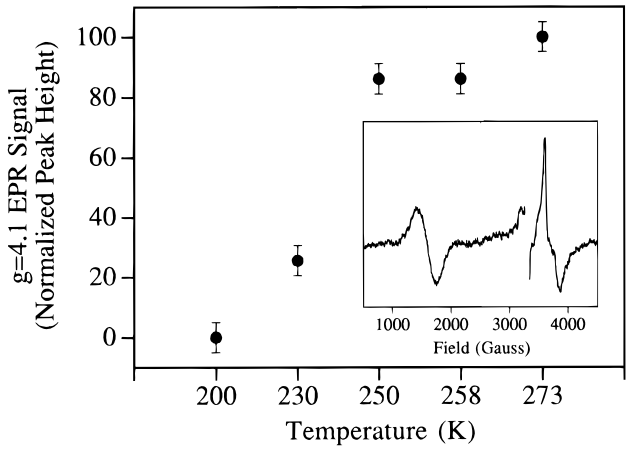

FIGURE 6: Yields of the S_2-state $g = 4.1$ EPR signal in DCMU- and acetate-treated PSII as a function of illumination temperature. Illumination times were the following: 230 K, 5 min; 250 K, 5 min; 258 K, 30 s; 273 K, 15 s. The sizes of the error bars are based on measurement of the signal-to-noise ratio for the EPR spectra. Inset: light-minus-dark difference spectrum showing the S_2-state $g = 4.1$ and $g = 1.9$ $Fe^{2+}Q_A^-$ EPR signals produced by 273 K illumination of DCMU- and acetate-treated PSII.

model predicts the exclusive formation of the S_2-state $g = 4.1$ EPR signal in acetate- and DCMU-treated PSII as observed, it does not explain why an S_2-state multiline EPR signal is observed in acetate- and NO•-treated PSII once the interaction with Y_Z• has been removed.

Figure 5 addresses this question by showing that when PSII treated only with acetate was illuminated at 294 K, both the S3 EPR signal and a multiline EPR signal were observed (spectrum b). The splittings and peak positions of the multiline signal found in acetate-treated PSII were almost identical to those found for the S_2-state multiline EPR signal in untreated PSII. The intensity was approximately 15% of the yield of the S_2-state multiline EPR signal induced in DCMU-treated PSII illuminated at 200 K. This yield of the S_2-state multiline EPR signal is not due to a small fraction of untreated centers since it was not observed upon 200 K illumination of acetate-treated PSII or upon 273 K illumination of acetate- and DCMU-treated PSII (Figure 6, inset). The fact that a small steady-state amount of S_2-state multiline EPR signal was observed when the S3 EPR signal was present implicates the multiline form of the S_2 state in the formation and/or decay pathway of the S3 EPR signal (see eq 2).

DISCUSSION

Our results on binding NO• to PSII have confirmed some of the earlier results of Petrouleas and Diner (1990). As reported, we found that the EPR signal from Y_D• is reversibly quenched by NO• and that the recovered yield upon removal of NO• in the dark is high (Figure 1). On the basis of recent results on the binding of NO• to the tyrosyl radical in ribonucleotide reductase, the binding of NO• to Y_D• in PSII is probably similar and occurs through formation of a weak bond of the tyrosyl radical oxygen atom with NO• (Figure 7). In addition to the studies on Y_D•, we have also shown that, by using illumination conditions designed to trap Y_Z• (Tang et al., 1996b), no EPR signal from Y_Z• is observed in manganese-depleted samples treated with NO• (Figure 2). These results suggest that as soon as Y_Z• is formed, it reacts with NO• to form a diamagnetic Y_Z−NO adduct at a rate

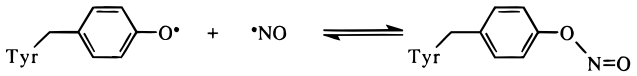

FIGURE 7: Proposed mode of NO• binding to tyrosyl radicals in PSII. A bent structure is expected if NO• is a one-electron donor to the tyrosyl radical.

faster than the decay reactions of Y_Z•. Upon removal of NO• in the dark, Y_Z• can be formed by reilluminating the sample. Interestingly, it appears that both the Y_D−NO and Y_Z−NO adducts are resistant to oxidation by $P680^+$ since we observed no new organic radical EPR signals attributable to oxidized forms of the Y_Z−NO and Y_D−NO adducts.

Since Y_Z• has been identified as the radical giving rise to the S3 EPR signal (Gilchrist et al., 1995; Tang et al., 1996a) and Y_Z• binds NO•, we were interested in using NO• as a spin probe to characterize the S3 EPR signal in acetate-treated PSII. In acetate-treated PSII samples illuminated under conditions that produce the highest yield of the S3 EPR signal, no S3 EPR signal was observed in the presence of NO• (Figure 4). When the NO• was removed in the dark and the sample was reilluminated, the S3 EPR signal appeared with a yield comparable to that found for the acetate-treated PSII which had not been incubated with NO•. We conclude that the S3 EPR signal is not observed when NO• is present because NO• reacts with the radical producing the S3 EPR signal to form a diamagnetic species (see eq 1).

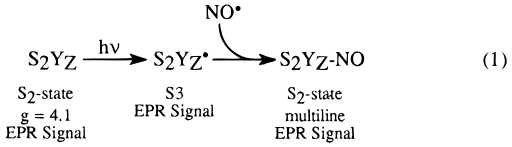

(1)

In order for NO• to trap Y_Z•, NO• binding must occur within the lifetime of Y_Z• (see eq 1). For manganese-depleted samples, Y_Z• was stably trapped by freezing under illumination (Figure 2b). The fact that NO• completely suppressed formation of the Y_Z• EPR signal requires that the binding of NO• must be fast relative to both the decay of Y_Z• and the rate of freezing. An upper limit on the time required for NO• to bind to Y_Z• at room temperature can be estimated from the rate of charge recombination of Y_Z• with Q_A^- which has a half-time of 430 ms in Tris-treated spinach PSII at pH 7.5 (Dekker et al., 1984a). On the other hand, we observed the formation of an S_2-state multiline EPR signal in acetate-treated samples containing NO•, which requires that the samples are capable of advancing from the S_1 to the S_2 state in the presence of NO•. Therefore, the rate of NO• binding to Y_Z• in acetate- and NO•-treated samples must be slower than the 70−110 μs half-time for reduction of Y_Z• by the S_1 state (Hoganson and Babcock, 1988). An additional consideration in acetate-treated samples is that S-state turnover is blocked after the S_2 state. This means that binding of NO• to S_2Y_Z• may occur in acetate-treated PSII due to the longer lifetime of Y_Z• since the half-time for Y_Z•Q_A^- charge recombination has been measured to be greater than 100 ms in acetate-treated PSII from *Synechococcus* (Bock et al., 1988).

The estimates of the rates of NO• binding to Y_Z• outlined above suggest the possibility of using NO• to trap higher S states in otherwise untreated PSII. Since the reaction between Y_Z• and NO• is bimolecular, the rate of the reaction can be directly affected by increasing the concentration of NO•. By controlling the rate of reaction in this manner, it may be possible to trap the S_3 state since the S_3 to S_0 transition of the OEC has been estimated to occur with a half-time of approximately 1 ms (Hoganson and Babcock, 1988). Experiments using high concentrations of NO• may increase the rate enough to allow NO• to bind to Y_Z• to form the state S_3Y_Z−NO.

Since the S3 EPR signal species has been described as the state S_2X^+, quenching of the organic radical species X^+ could facilitate observation of an EPR signal from the S_2 state. Indeed, formation of the diamagnetic Y_Z−NO adduct by illumination of acetate-treated PSII incubated with NO• revealed an S_2-state multiline EPR signal. We also observed a small amount of an S_2-state multiline EPR signal in PSII treated only with acetate. In their work on acetate-treated PSII, MacLachlan et al. (1993) reported small satellite peaks associated with the S3 EPR signal and described them as being part of the S3 EPR signal (MacLachlan and Nugent, 1993). We attribute these smaller peaks to some S_2-state multiline EPR signal which has been trapped during the continuous illumination used to produce the S3 EPR signal (see eq 2). This means that the rate of photo-oxidation of

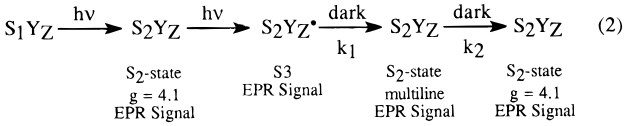

(2)

Y_Z is on the same time scale as the conversion of the multiline form of the S_2 state back to its $g = 4.1$ form (rate constant k_2 in eq 2). In this case, a small steady-state yield of the S_2-state multiline EPR signal could be trapped during the formation of the S3 EPR signal and the low yield of the S_2-state multiline EPR signal found in acetate-treated PSII samples exhibiting an S3 EPR signal can be explained by the competing formation and decay reactions involved in generation of the S3 EPR signal species.

The model shown in eq 2 also suggests that the oxidation of Y_Z is coupled to the observed S_2-state conformational change. Oxidation of Y_Z is expected to result in loss of a hydrogen bond in the vicinity of Y_Z. Since Y_Z has been proposed to be close to the OEC (Gilchrist et al., 1995), it may be that the rearrangement of the OEC in the S_2 state is due to the loss of a hydrogen bond between Y_Z and the OEC. It has been argued that Y_Z is directly involved in substrate activation through hydrogen atom or proton abstraction (Gilchrist et al., 1995; Hoganson et al., 1995). Our observation that an S_2-state conformational change occurs upon oxidation of Y_Z to form the S3 EPR signal is consistent with this model for the function of Y_Z. If advancement to the S_3 state is tied to the proton-coupled reduction of Y_Z•, S-state turnover would be blocked in any inhibited PSII sample where hydrogen bonding and the substrate-binding site have been disrupted.

Why is acetate-inhibited PSII unable to advance beyond the state S_2Y_Z•? Several models have recently been proposed in which Y_Z• acts as a hydrogen atom or proton abstractor from the Mn_4 cluster (Gilchrist et al., 1995; Hoganson et al., 1995). However, these models do not discuss the possible role of reduction potential differences between Y_Z• and the S states of the Mn_4 cluster. During S-state turnover, the reduction potential of the Mn_4 cluster is expected to increase upon each S-state advance. By using the reduction

potential of $Y_D^{\bullet}$ as a reference point, it is known that the S_2 and S_3 states have higher reduction potentials than the S_1 state because $Y_D^{\bullet}$ oxidizes the S_0 state, but the S_2 and S_3 states oxidize Y_D to $Y_D^{\bullet}$ (Vass and Styring, 1991). Based on analyses of electron-transfer kinetics on the donor side of PSII and on charge-recombination reactions, the reduction potentials of the Mn_4 cluster have been concluded to increase progressively with increasing S state (Buser et al., 1992; Shinkarev & Wraight, 1993, and references therein). If this is the case, how does $Y_Z^{\bullet}$ remain a competent oxidant of the Mn_4 cluster if its reduction potential remains constant during S-state turnover? This question can be addressed by assuming that the driving force for each S-state advance can be divided into energy contributions from the electron-transfer reaction and from bond-breaking/bond-making processes. As long as the reduction potential for an S-state transition is not too high, $Y_Z^{\bullet}$ will be able to oxidize the Mn_4 cluster by an outer-sphere electron-transfer process. This is likely to be the case for the lower S states. However, in the higher S states, the reduction potential of the Mn_4 cluster may be too high for a simple outer-sphere electron transfer to $Y_Z^{\bullet}$ to be energetically downhill. In this case, the extra free energy derived from forming the phenoxyl−OH bond may be crucial for the S-state transition to occur (eq 3).

$$S_2(\text{hydroxo})\ {}^{\bullet}\text{O-Tyr} \longrightarrow S_3(\text{oxo})\ \text{HO-Tyr} \qquad (3a)$$

$$S_2(\text{acetate})\ {}^{\bullet}\text{O-Tyr} \longrightarrow \text{no reaction} \qquad (3b)$$

The reduction potential of $Y_Z^{\bullet}/Y_Z$ has been estimated to be between 1.0 and 1.1 V (Buser et al., 1992, and references therein). Some hydrogen atom transfer effects are probably included in the estimate of the $Y_Z^{\bullet}$ reduction potential since it is somewhat higher than the measured 890 mV reduction potential for the tyrosyl radical/tyrosinate couple at pH 7.0 (Lind et al., 1990). The midpoint potentials of the S_0 to S_1 and the S_1 to S_2 transitions have been estimated to be about 700 and 900 mV, respectively (Buser et al., 1992; Vass and Styring, 1991). Because the S_0 and S_1 states have lower potentials than the reduction potential of $Y_Z^{\bullet}$, the overall free energy change for S-state advance is negative and, therefore, energetically favorable when only the electron-transfer event is considered. However, once the S_2 state has been reached, the energy difference between the S_2 state and $Y_Z^{\bullet}$ may approach zero since the potential of the S_2 state has been estimated to be very close to 1.0 V (Buser et al., 1992). At this stage, a direct proton-coupled electron transfer from the Mn_4 cluster to $Y_Z^{\bullet}$ may become critical in maintaining the driving force for S-state advance. This is not unreasonable since proton-coupled electron-transfer reactions have been observed to significantly affect the reduction potentials of binuclear manganese−oxo complexes (Thorp et al., 1989).

Since a proton-coupled electron-transfer reaction for the reduction of $Y_Z^{\bullet}$ could be a crucial component of the driving force for the water oxidation chemistry in the higher S states, it is important to evaluate the energies of the bonds that are broken and formed. As a rough approximation, the contribution of bond energies to the driving force for the reduction of $Y_Z^{\bullet}$ by proton-coupled electron transfer from the Mn_4 cluster can be estimated by a comparison of the OH bond strengths of the two species. Using a di-μ-oxo-bridged manganese dimer as a model, the bond strength of a manganese−OH bond can be estimated to be 82 kcal/mol (Gardner & Mayer, 1995; Manchanda et al., 1992). The bond strength of a tyrosine−OH bond is 86.5 kcal/mol (Lind et al., 1990). With these estimates, the bond energies would provide approximately 4.5 kcal/mol or 195 mV to the driving force for the reaction. This contribution to the driving force for the electron-transfer reaction is significant and may explain why inhibited PSII samples cannot advance beyond the S_2 state. Like acetate, other inhibitory treatments may block proper binding of substrate to the OEC. Perturbation of hydrogen bonding between the Mn_4 cluster and Y_Z could explain why many treatments result in formation of the state $S_2Y_Z^{\bullet}$ and observation of the S3 EPR signal.

ACKNOWLEDGMENT

We thank R. David Britt for sending copies of several manuscripts prior to publication.

REFERENCES

Andréasson, L.-E., & Lindberg, K. (1992) *Biochim. Biophys. Acta 1100*, 177−183.
Arnon, D. I. (1949) *Plant Physiol. 24*, 1−15.
Baumgarten, M., Philo, J. S., & Dismukes, G. C. (1990) *Biochemistry 29*, 10814−10822.
Beck, W. F., de Paula, J. C., & Brudvig, G. W. (1985) *Biochemistry 24*, 3035−3043.
Berthold, D. A., Babcock, G. T., & Yocum, C. F. (1981) *FEBS Lett. 134*, 231−234.
Bock, C. H., Gerken, S., Stehlik, D., & Witt, H. T. (1988) *FEBS Lett. 227*, 141−146.
Boussac, A., & Rutherford, A. W. (1988) *Biochemistry 27*, 3476−3483.
Boussac, A., Zimmermann, J.-L., & Rutherford, A. W. (1989) *Biochemistry 28*, 8984−8989.
Boussac, A., Zimmermann, J.-L., Rutherford, A. W., & Lavergne, J. (1990) *Nature (London) 347*, 303−306.
Buser, C. A., & Brudvig, G. W. (1992) in *Current Research in Photosynthesis* (Murata, N., Ed.) pp 85−88, Kluwer Academic Publishers, Dordrecht, The Netherlands.
Buser, C. A., Diner, B. A., & Brudvig, G. W. (1992) *Biochemistry 31*, 11449−11459.
Debus, R. J. (1992) *Biochim. Biophys. Acta 1102*, 269−352.
De Groote, M. A., Granger, D., Xu, Y., Campbell, G., Prince, R., & Fang, F. C. (1995) *Proc. Natl. Acad. Sci. U.S.A. 92*, 6399−6403.
Dekker, J. P., van Gorkom, H. J., Brok, M., & Ouwehand, L. (1984a) *Biochim. Biophys. Acta 764*, 301−309.
Dekker, J. P., van Gorkom, H. J., Wensink, J., & Ouwehand, L. (1984b) *Biochim. Biophys. Acta 767*, 1−9.
Gardner, K. A., & Mayer, J. M. (1995) *Science 269*, 1849−1851.
Gaston, B., Reilly, J., Drazen, J. M., Fackler, J., Ramdev, P., Arnelle, D., Mullins, M. E., Sugarbaker, D. J., Chee, C., Singel, D. J., Loscalzo, J., & Stamler, J. S. (1993) *Proc. Natl. Acad. Sci. U.S.A. 90*, 10957−10961.
Ghanotakis, D. F., & Yocum, C. F. (1990) *Annu. Rev. Plant Physiol. Plant Mol. Biol. 41*, 255−276.
Gilchrist, M. L., Lorigan, G. A., & Britt, R. D. (1995) *Proc. Natl. Acad. Sci. U.S.A. 92*, 9545−9549.
Guiles, R. D., Zimmermann, J.-L., McDermott, A. E., Yachandra, V. K., Cole, J. L., Dexheimer, S. L., Britt, R. D., Wieghardt, K., Bossek, U., Sauer, K., & Klein, M. P. (1990) *Biochemistry 29*, 471−485.
Hoganson, C. W., & Babcock, G. T. (1988) *Biochemistry 27*, 5848−5855.
Hoganson, C. W., Lydakis-Simantiris, N., Tang, X.-S., Tommos, C., Warncke, K., Babcock, G. T., Diner, B. A., McCracken, J., & Styring, S. (1995) *Photosynth. Res. 46*, 177−184.
Janzen, E. G., Wilcox, A. L., & Manoharan, V. (1993) *J. Org. Chem. 58*, 3597−3599.
Jia, L., Bonaventura, C., Bonaventura, J., & Stamler, J. S. (1996) *Nature (London) 380*, 221−226.

Kok, B., Forbush, B., & McGloin, M. (1970) *Photochem. Photobiol. 11*, 457.
Lepoivre, M., Flaman, J.-M., & Henry, Y. (1992) *J. Biol. Chem. 267*, 22994−23000.
Lind, J., Shen, X., Eriksen, T. E., & Merényi, G. (1990) *J. Am. Chem. Soc. 112*, 479−482.
MacLachlan, D. J., & Nugent, J. H. A. (1993) *Biochemistry 32*, 9772−9780.
Manchanda, R., Thorp, H. H., Brudvig, G. W., & Crabtree, R. H. (1992) *Inorg. Chem. 31*, 4040−4041.
Miyao, M., & Murata, N. (1984) *FEBS Lett. 170*, 350−354.
Nugent, J. H. A., MacLachlan, D. J., Rigby, S. E. J., & Evans, M. C. W. (1993) *Photosynth. Res. 38*, 341−346.
Ono, T., & Inoue, Y. (1990) *Biochim. Biophys. Acta 1020*, 269−277.
Ono, T., Noguchi, T., Inoue, Y., Kusunoki, M., Matsushita, T., & Oyanagi, H. (1992) *Science 258*, 1335−1337.
Petrouleas, V., & Diner, B. A. (1990) *Biochim. Biophys. Acta 1015*, 131−140.
Roy, B., Lepoivre, M., Henry, Y., & Fontecave, M. (1995) *Biochemistry 34*, 5411−5418.
Rutherford, A. W., Zimmermann, J.-L., & Boussac, A. (1992) in *The Photosystems: Structure, Function, and Molecular Biology* (Barber, J., Ed.) pp 179−229, Elsevier Science Publishers, Amsterdam.
Shinkarev, V. P., & Wraight, C. A. (1993) *Proc. Natl. Acad. Sci. U.S.A. 90*, 1834−1838.
Sinclair, J. (1984) *Biochim. Biophys. Acta 764*, 247−252.
Sivaraja, M., Tso, J., & Dismukes, G. C. (1989) *Biochemistry 28*, 9459−9464.
Stamler, J. S., Jaraki, O., Osborne, J., Simon, D. I., Keaney, J., Vita, J., Singel, D., Valeri, C. R., & Loscalzo, J. (1992a) *Proc. Natl. Acad. Sci. U.S.A. 89*, 7674−7677.
Stamler, J. S., Simon, D. I., Osborne, J. A., Mullins, M. E., Jaraki, O., Michel, T., Singel, D. J., & Loscalzo, J. (1992b) *Proc. Natl. Acad. Sci. U.S.A. 89*, 444−448.
Svensson, B., Vass, I., & Styring, S. (1991) *Z. Naturforsch. 46C*, 765−776.
Szalai, V. A., & Brudvig, G. W. (1996) *Biochemistry 35*, 1946−1953.
Tamura, N., & Cheniae, G. (1987) *Biochim. Biophys. Acta 890*, 179−194.
Tanaka, S., & Wada, K. (1988) *Photosynth. Res. 17*, 255−266.
Tang, X.-S., Randall, D. W., Force, D. A., Diner, B. A., & Britt, R. D. (1996a) *J. Am. Chem. Soc. 118*, 7638−7639.
Tang, X.-S., Zheng, M., Chisholm, D. A., Dismukes, G. C., & Diner, B. A. (1996b) *Biochemistry 35*, 1475−1484.
Thompson, L. K., & Brudvig, G. W. (1988) *Biochemistry 27*, 6653−6658.
Thorp, H. H., Sarneski, J. E., Brudvig, G. W., & Crabtree, R. H. (1989) *J. Am. Chem. Soc. 111*, 9249−9250.
Vass, I., & Styring, S. (1991) *Biochemistry 30*, 830−839.
Wilcox, A. L., & Janzen, E. G. (1993) *J. Chem. Soc., Chem. Commun.* 1377−1379.
Zimmermann, J.-L., Boussac, A., & Rutherford, A. W. (1993) *Biochemistry 32*, 4831−4841.

BI961117W